Combined Cryo and Room-Temperature Ball Milling to Produce Ultrafine Halide Crystallites

AKASH VERMA, KRISHANU BISWAS, CHANDRA SEKHAR TIWARY, AMIT KUMAR MONDAL, and KAMANIO CHATTOPADHYAY

The combined milling at cryogenic temperature as well as room temperature (RT) has been carried out to prepare ultrafine NaCl crystallites. The milling has been done in evacuated tungsten carbide vials backfilled with high-purity Ar. The results indicate the effect duration of cryomilling prior to RT milling has a strong effect on the final crystallite size. The deformation aided sintering of NaCl crystallites during RT milling and leads to the formation of bimodal distribution of crystallites. The cuboidal-shaped NaCl crystallite undergoes a roughening transition due to plastic deformation. The experimental results are explained using the temperature-dependent mechanical properties of NaCl single crystals and plastic-deformation-induced roughening.

DOI: 10.1007/s11661-010-0490-1

I. INTRODUCTION

NANOCRYSTALLINE materials constitute an important class of materials. The sole characteristic of nanomaterials is the size effect *i.e.*, the properties of these materials depend on the crystallite size or grain size. The preparation and characterization of these novel materials is very much needed to probe the effect of size on the properties. These materials can be synthesized by using either the bottom-up or the top-down approach.[1] The bottom-up approach refers to the build up of the nanomaterials from the bottom; atom-by-atom, layer-by-layer or cluster-by-cluster. In the top-down approach the micron- or submicron-sized microstructure changes to nanostructures for the bulk material. Attrition or mechanical milling is a typical top-down method in preparing nanoparticles.

The communition of powders to a small size by using high-energy ball-milling is termed mechanical milling.[2–5] The process is carried out in a high-energy ball mill, and it involves repeated deformation, cold-welding, fracturing, and dynamic recrystallization to achieve an extremely fine grain size.[2] The force of the impact exerted by the balls plastically deforms the power leading to work hardening and fracture. The main attribute of this process is the refinement of crystallite size to nanometric range. The biggest disadvantage with the top-down approach is the generation of structural defects in the material. Substantial amount of research work has been done in preparation and in characterization of metallic, oxide, nitride, and carbide nanoparticles.[1] To the best of the authors' knowledge, there is no research work available dealing with preparation and characterization of ultrafine halide nanoparticles. The halides are very reactive and thus these nanoparticles cannot be prepared using bottom-up methods. One needs to use the top-down approach to synthesize these nanoparticles.

The present article deals with the preparation and detailed characterization of sodium chloride nanoparticles by combined low temperature (cryo) and room-temperature (RT) vacuum milling.[3–5] Cryomilling is a variation of mechanical milling in which metallic or ceramic powders are milled in cryogenic slurry (liquid N_2) or at cryogenic temperatures such that nanostructures are obtained. It is well known that the cooling of powders is an effective way to accelerate the fracturing process.[3–5] In addition, extremely low temperatures in cryomilling suppress recovery and recrystallization processes, causing rapid grain refinement.[4,5] It has been reported[2,4,5] that the ultimate grain size achieved by mechanical milling is dictated by balance between two factors: (1) defect creation and (2) recovery during plastic deformation. Therefore, for any material with faster recovery, it is difficult to attain a sufficiently high defect accumulation for grain refinement. The recovery kinetics is a strong function of temperature. It is well known that dynamic recovery can be suppressed effectively by low-temperature milling for many materials. The defect generation also depends on milling temperature. At an extremely low temperature, the plastic deformation is limited, and therefore, defect generation is not sufficient to obtain a finer grain size. On other hand, RT milling will lead to the generation as well as annihilation of defects such as dislocations. Therefore, it is expected that combined cryo and RT milling will cause a refinement of grain size. In the present investigation, such a study is carried out on NaCl, which is extremely brittle at low temperature.

AKASH VERMA, Student, and KRISHANU BISWAS, Assistant Professor, are with the Department of Materials Science and Engineering, Indian Institute of Technology, Kanpur, U.P. 208016, India. Contact e-mail: kbiswas@iitk.ac.in CHANDRA SEKHAR TIWARY, Student, AMIT KUMAR MONDAL, Project Associate, and KAMANIO CHATTOPADHYAY, Professor, are with the Department of Materials Engineering, Indian Institute of Science, Bangalore, Karnataka 560012, India.

Manuscript submitted April 4, 2010.
Article published online November 4, 2010

There are several stages of evolution of powder during mechanical milling.[5] During the first stage, the powder undergoes extensive plastic deformation, which is localized into shear bands. For ductile materials, the extensive deformation may lead to the formation of flattened particles, which can even get welded. In the subsequent stage, the defects forming in the shear bands are accumulated to form subgrains within large grains. These subgrains are separated by low-angle grain boundaries. In the later stages, further deformation will cause a multiplication of shear bands with further reduction of subgrains. Finally, the reorientation of final grains with high-angle grain boundaries occurs.

II. EXPERIMENTAL METHODS

Pure NaCl powder (Merck, Damstadt, Germany) was ball milled in a modified P0 (Pulverisette) mill using four 15-mm diameter tungsten carbide (WC) balls in a WC vial. The ball-to-powder weight ratio was kept as 20:1 at low temperature (77 K (−196 °C)) as well as RT. The low temperature was created by pouring a mixture of liquid nitrogen (LN_2) and methane in an annular jacket around the vial. The powder in the vial was not in contact with the LN_2, thereby there was no contamination from coolant. The temperature of the sample was measured by a resistance temperature detector (RTD) probe attached to the vial. The vials loaded with the powder and ball were evacuated using a vacuum pump to a pressure of 10^{-2} mbar before backfilling with argon gas. Milling was stopped intermittently to ensure the vacuum in the vial. Cryomilling times ranged from a few minutes to 8 hours. The RT milling was carried out in the same mill with the same milling parameters. The milling time in RT milling varied from a few hours to 20 hours. The samples taken out at different time durations were stored in the vacuum desiccators with kerosene to prevent oxidation. Sufficient care had been taken to ensure that no contamination took place during milling.

The milled powders were examined by X-ray diffraction (XRD) technique using a Pan analytical Xpert Pro X-ray powder diffractometer (PANalytical B.V., Almelo, The Netherlands) with CuK_α radiation ($\lambda = 0.154056$ nm). The peak shift was corrected using Si as an external standard. Microstructural analysis was performed using a scanning electron microscope (SEM, FEI SIRION XL 40 SFEG) operating at 5 kV as well as a transmission electron microscope (TEM, Technai F30) operating at 100 kV. As radiation damage has always been a problem for the observation of NaCl in TEM,[6] sufficient care had been taken to minimize radiation damage. The milled NaCl powders were mounted on a Cu-grid of high mesh number (600 mesh size) so that charging could be avoided. Working quickly at a low intensity (smaller condenser aperture) and at a lower accelerating voltage had not been sufficient to obtain good quality images with minimum radiation damage. The samples were cooled to liquid nitrogen temperature using a cryoholder (Gaton, PA) to obtain good quality images.

III. RESULTS AND DISCUSSION

A. *XRD*

Figure 1 shows X-ray diffraction patterns of NaCl powder cryomilled as well as RT milled as a function of milling time. The milling conditions are written against each diffraction pattern. The vertical lines in the bottom of the figure indicate the position of NaCl, Si peaks as per the International Committee for Diffraction Data database. As already mentioned, Si is used as an external standard. The XRD patterns clearly indicate the presence of NaCl and Si peaks only. We have not observed peaks from any contaminants.

B. *SEM Observation*

We shall now discuss the microstructural evolution of the ball-milled powder using SEM. The process of mechanical milling of powder normally involves repeated welding, fracturing, and rewelding of powder particles. This process leads to the reduction of crystallite size caused by plastic deformation.[2,4,5] Figure 2 shows SEM micrographs of NaCl samples, revealing the information about the nature of particles when cryomilled for 2, 4, and 8 hours. Figure 2(a) is the micrograph of the starting powder showing large (50 to 100 μm) cuboidal-shaped NaCl crystallites bounded by {100} facets. As compared with the starting microstructure, several important characteristics can be observed in cryomilled powder. Figure 2(b) shows a SEM micrograph of a sample cryomilled for 2 hours. Most NaCl crystallites have undergone fracturing (marked by white arrows) leading to the formation of fragmented crystallites. The cuboidal shape of the starting crystallite is still retained. Cryomilling leads to a decrease of crystallite size (1–2 μm) as shown in the inset of Figure 2(b) revealing small crystallites. Figure 2(c) reveals the representative micrograph of 4 hours cryo-milled sample. The crystallites have further been fractured and fragmented pieces can be clearly observed. However, some

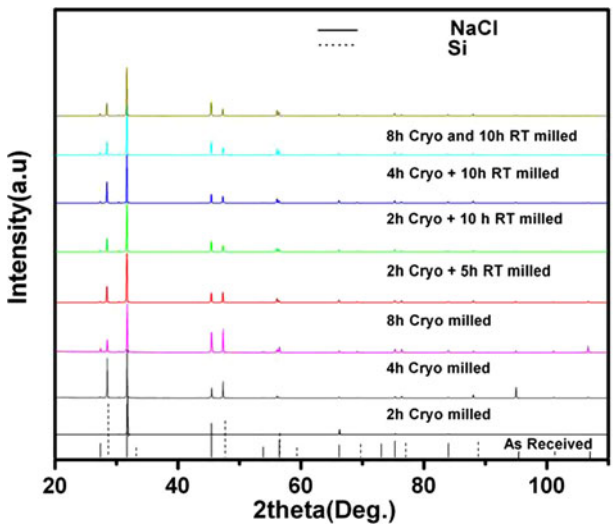

Fig. 1—XRD patterns of the NaCl milled at different times using cryo and RT milling.

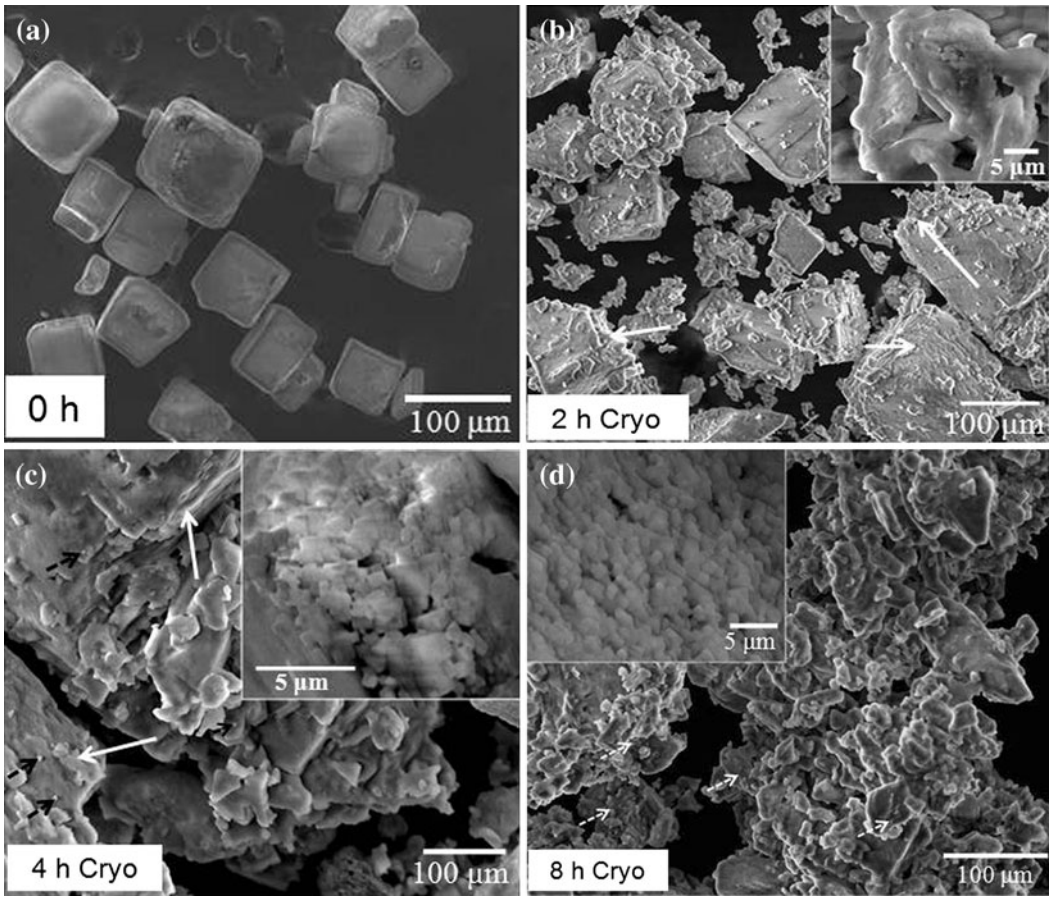

Fig. 2—SEM microstructure of cryomilled samples for different time scales: (*a*) 0 h; (*b*) 2 h (*c*) 4 h, and (*d*) 8 h. The insets in (*b*), (*c*), and (*d*) show higher magnification micrographs.

facets of the crystallite are still retained (marked by white arrows). The formation of finer scale cuboidal-shaped NaCl crystallites can also be observed on surface of the fractured crystallites as indicated by dotted black arrows. The inset shows higher magnification micrograph of these particles with facets. SEM micrograph of the 8-hour cryomilled sample is shown in Figure 2(d). The original cuboidal-shaped NaCl crystallites are not observed in the microstructure. The larger crystallites (as observed in the 4-hours milled sample) are completely fragmented leading to the formation of smaller crystallites, which are marked by dotted white arrows. The inset shows the formation of finer-scale crystallites (~1 μm). Further cryomilling does not lead to a change in the microstructure as well as in the crystallite sizes.

We shall now discuss SEM observation of the cryomilled samples which are subsequently RT milled for different time scale. We shall present some representative SEM micrographs. Figure 3(a) is the SEM micrograph of sample cryomilled for 2 hours and subsequently RT milled for 5 hours. The micrograph illustrates the bimodal distribution of the crystallites. The crystallites have a typical cuboidal morphology (marked by white arrow). The inset shows the finer scale crystallites along with the bigger faceted NaCl crystallites. Some of these bigger crystallites have well-developed facets. The SEM micrograph of sample cryomilled for 2 hours and RT milled for 10 hours is shown in Figure 3(b). The microstructure again shows a bimodal distribution of the NaCl crystallite with bigger crystallites showing pronounced faceting. It is clear that longer RT milling leads to further reduction of crystallites. However, the crystallite undergoes a morphological change from a cuboidal to a cuboctahedron shape. The SEM microstructure of a sample cryomilled for 4 hours and RT milled for 10 hours is shown in Figure 3(c). The size of the crystallites has indeed been reduced as compared to the earlier two cases. The shapes of the crystallites have been changed to cuboctahedral-shaped crystallites (marked by a black arrow). Figure 3(d) shows a SEM micrograph of the sample cryomilled for 8 hours and subsequently RT milled for 10 hours. The crystallite size has been reduced much finer scale and the shape of the crystallites has been changed. Some crystallites have a near spherical shape. The inset of Figure 3(d) shows a high magnification micrograph of a crystallite with a near spherical shape.

C. *TEM Observation*

We have carried out a detailed TEM study of all samples. Radiation damage during TEM observation was always a problem.[6] The TEM was operated at

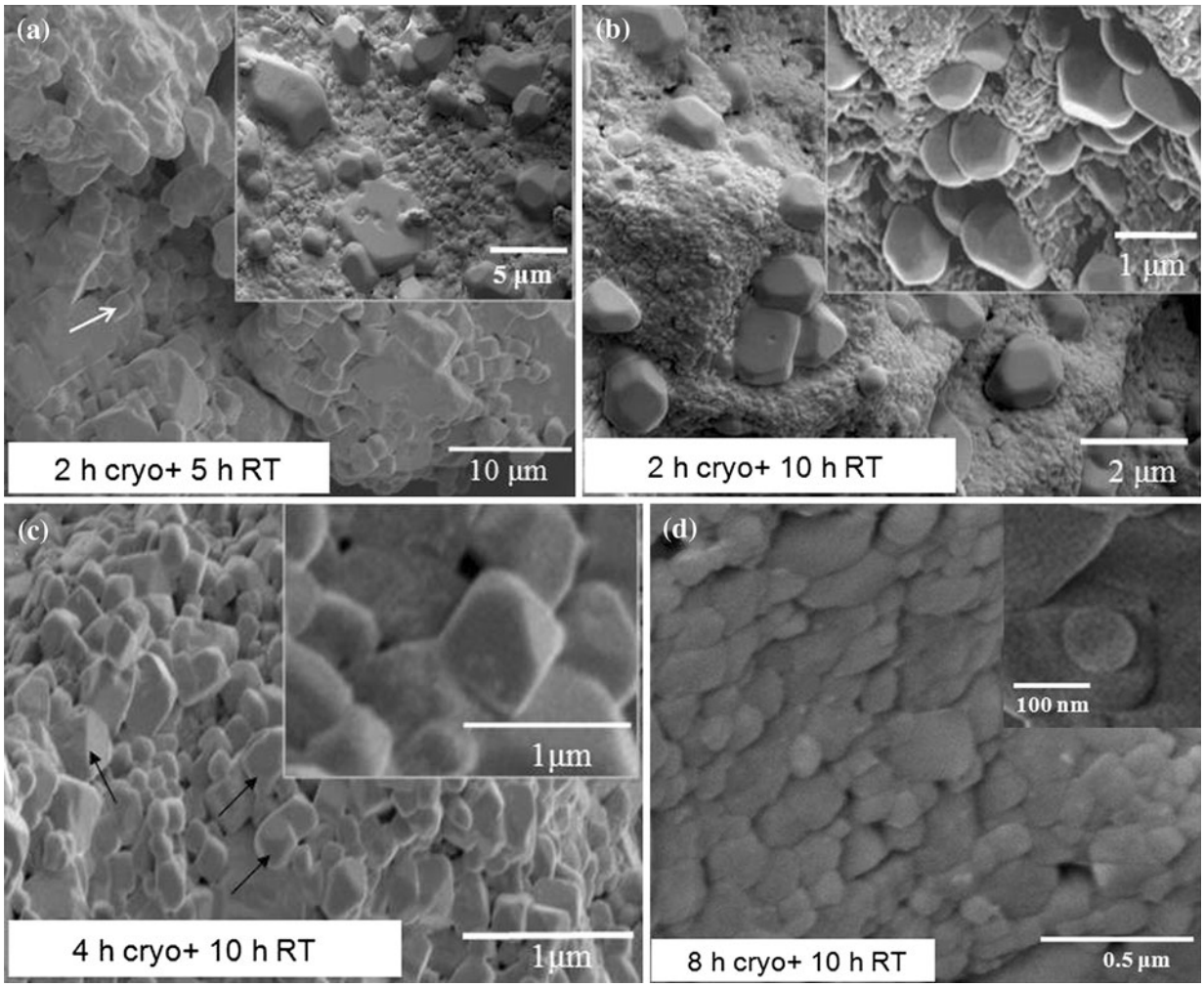

Fig. 3—SEM images of milled powder: (*a*) 2 h of cryomilling with 5 h of RT milling, (*b*) 2 h of cryomilling and 10 h of RT milling, (*c*) 4 h cryomilling and 10 h of RT milling, and (*d*) 8 h of cryomilling and 10 h of RT milling.

100 KV with minimum beam current. The smaller condenser aperture was usually 2 μm, and the first condenser aperture was fully excited to obtained minimum beam diameter on the specimen to minimize beam-induced volatilization. We shall present here representative micrographs obtained from different samples. Figure 4(a) is a typical bright-field micrograph of a sample cryomilled for 2 hours revealing different NaCl crystallites. The top inset is a high-magnification bright-field micrograph of one such crystallite oriented along the [001] direction. The crystallite is found bounded by {100} facets. The particle size distribution has been shown as the bottom inset of Figure 4(a). The average crystallite size is 150 ± 40 nm. There are few crystallites in the size range of 20–100 nm. Figure 4(b) shows a bright-field micrograph of powder cryomilled for 4 hours. The top inset shows higher magnification bright-field micrograph of one of the crystallites (size ~80 nm). The micrograph has been obtained by orienting the particle along the [001] zone axis. It can be clearly observed that the two of the {100}-type facets have been roughened while other two have retained the sharpness. The bright-field micrograph of 8 hours cryo milled sample is shown in Figure 4(c). The crystallite size indeed has reduced during milling. The average crystallite size is 90 ± 14 nm. The large fraction of crystallites have a size <100 nm. A higher magnification micrograph of a crystallite of (size ~70 nm) is shown as an inset. It reveals {100} facets of the crystallites.

TEM observation of cryomilled and subsequently RT milled samples are shown in Figures 4(d) through (f). Figure 4(d) is a bright-field micrograph of powder cryomilled for 2 hours and subsequently RT milled for 10 hours. The crystallite size has been reduced substantially. The crystallite size distribution is shown in bottom inset of the figure. Measurements are carried on at least 100 crystallites using TEM bright-field micrographs to arrive at size distribution. The average crystallite size is 18 ± 11 nm. There are very few crystallites having size more than 30 nm. The upper inset shows a higher magnification bright-field micrograph of one of the crystallites (~35 nm). The micrograph has been obtained with the particle oriented along the [001] direction. It can be observed clearly that {100} facets of NaCl as observed in the starting powder, have been replaced by rough surfaces. Figure 4(e) reveals the

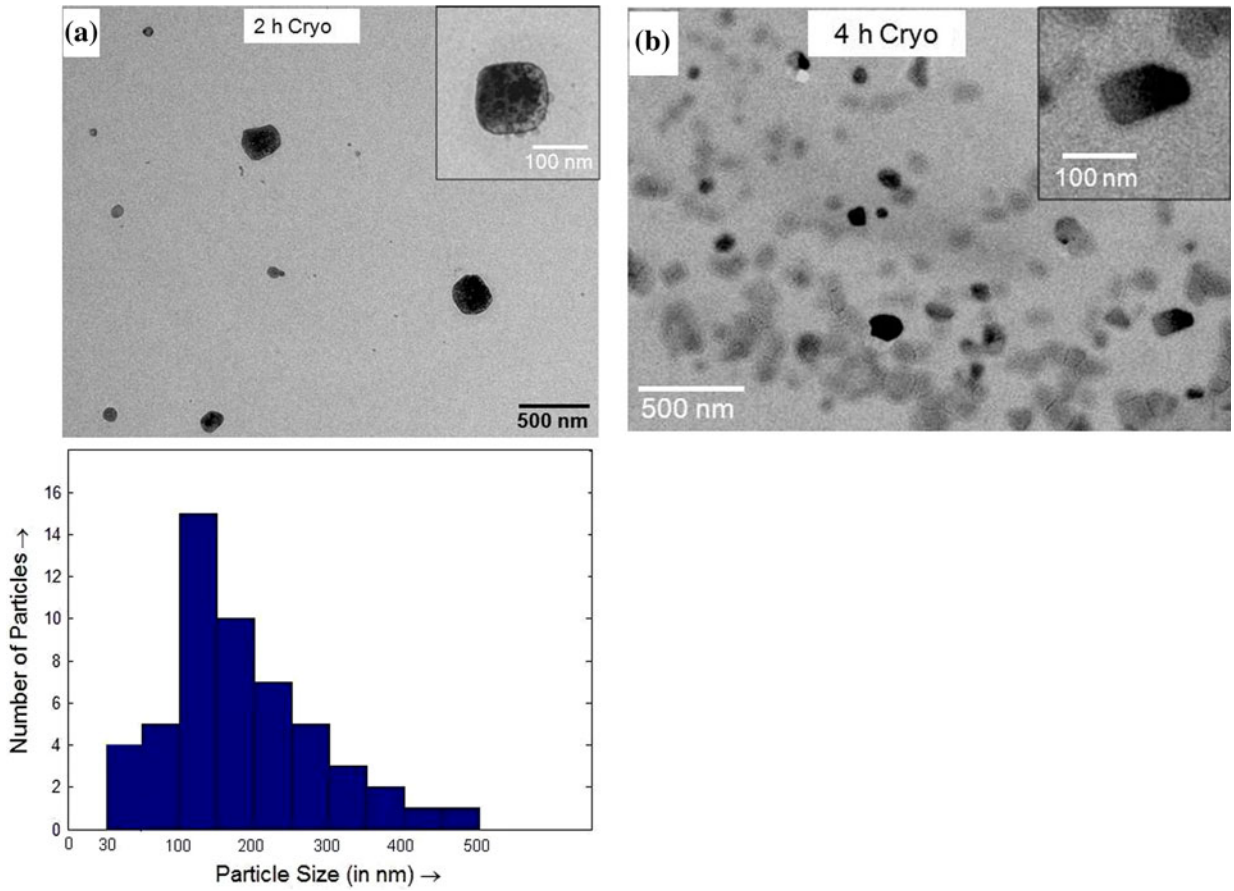

Fig. 4—TEM micrographs of milled powder: (*a*) 2 h of cryomilling, (*b*) 4 h of cryomilling; (*c*) 8 h cryomilling (*d*) 2 h of cryomilling and 10 h; (*e*) 4 h of cryomilling and 10 h of RT milling, and (*f*) 8 h of cryomilling and 10 h of RT milling. The top insets in each figure show higher magnification bright-field image of one crystallite oriented along the [001] direction. The bottom insets in figure (*a*) and (*c*) through (*e*) show the crystallite size distribution obtained from TEM micrographs.

bright-field micrograph of the sample cryomilled for 4 hours and subsequently RT milled for 10 hours. The bottom inset indicates the finer crystallite size distribution with an average size of 13 ± 7 nm. The top inset is a higher magnification micrograph of 8-nm-sized NaCl crystallite when the crystallite has been oriented along the [001] direction. One can clearly see that roughening of {100} facets. Figure 4(f) shows the bright-field micrograph of the sample cryomilled for 8 hours followed by RT milling for 10 hours. The crystallite size distribution, as shown in the bottom inset of Figure 3(e), demonstrates the distribution of fine crystallites (average = 9 ± 7 nm). The top inset shows a higher magnification bright-field micrograph of 8-nm-sized crystallites oriented along the [001] direction. The {100} facets are bounded rough surfaces. Figure 5 is a high-resolution image of NaCl nanocrystals. The image shows the presence of defects (as marked by white arrows) and surface steps.

IV. DISCUSSION

The current work has clearly shown that it is possible to prepare ultrafine nanocrystals of NaCl by combined milling at cryogenic temperatures and RT. The successful synthesis of large-scale nanostructured materials with ultrafine grain size is always considered as a major achievement in the field of nanotechnology. Preparation of nanostructured NaCl is important from a practical point of view because sintered NaCl performs are used in the manufacturing of highly porous microcellular metals or ceramics by replication process.[7] Nanosize NaCl crystallites definitely will improve the activity in the production of a porous structure. In addition, the nanostructured NaCl will have higher efficacy when used for medical purposes.[7]

During mechanical milling, the powder experiences severe plastic deformation, resulting in grain refinement.[3] It has been shown that the process basically leads to the transformation of a plastic-deformation-generated dislocation structure into high-angle grain boundaries.[2] According to Fecht,[8] microscopically, the formation of nanocrystalline material by mechanical milling involves three stages. In the first stage, severe plastic deformation is applied to the powder. The deformation thus induced is localized into shear bands containing a high-density network of dislocations. The plastic strain also is increased as a result of increasing dislocation density. In the second stage, due to a

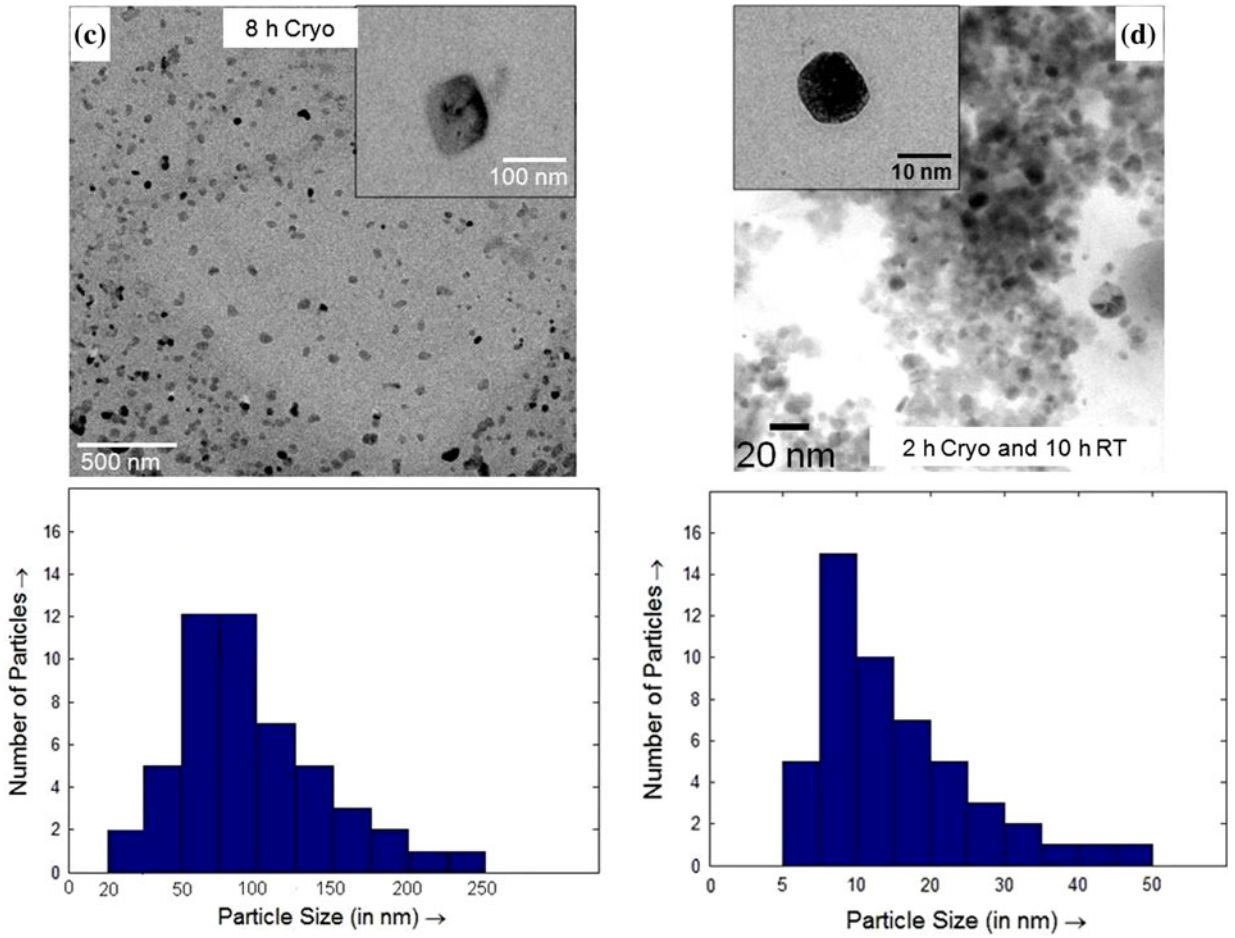

Fig. 4—Continued.

successive accumulation of the dislocations in the microstructure, the larger grains are disintegrated into subgrains separated by low-angle grain boundaries. The formation of these subgrains is attributed to the annihilation and recombination of dislocation by process of polygonization. In the final stage of mechanical milling, further deformation leads to the formation of additional shear bands with associated reduction of subgrain sizes and a reorientation of final grains with high-angle grain misorientation. The grain refinement during milling is achieved by the formation of shear bands under localized deformation followed by extension of the shear bands throughout the sample. Therefore, the dislocation generation and accumulation is the underlying necessity for grain refinement during mechanical milling. According to Mohamed,[9] the minimum grain size obtainable in any material basically is governed by two opposing factors: the hardening rate introduced by the dislocation generation and recovery rate due to dislocation annihilation and recombinations. Before we discuss the effect of combined cryo and RT milling on the formation of nanostructured NaCl, it is important to discuss its temperature-dependent mechanical property. For brittle materials, the factors leading to grain refinement during milling are temperature-enhanced deformation and microdeformation.[10,11]

Let us now discuss the mechanical properties of NaCl measured as a function of temperature reported in the literature.[12–14] NaCl is a brittle polycrystalline ceramic material at RT.[12–14] It has been found that it undergoes brittle-to-ductile transition at 540 K (267 °C).[12] In alkali-halides crystals with rock salt structure, slip operates on the $\{110\}\langle 1\bar{1}0\rangle$ system at RT and $\{010\}\langle 101\rangle$ system at high temperatures (>573 K [>300 °C]).[12–14] The fracture toughness of NaCl (K_{1C}) decreases slightly (from 0.2 MPa$\sqrt{m}$ to 0.1 MPa$\sqrt{m}$) as temperature increases from 77 K to 353 K (–196 °C to 80 °C) after a marked increase at a higher temperature.[12] Therefore, NaCl exhibits brittle behavior over a large temperature range (77 K to 353 K [–196 °C to 80 °C]) with negligible dislocation activity. It has already discussed that the fine-scale nanostructured NaCl crystallites cannot be prepared without build up of plastic-deformation-induced dislocation structure. Most importantly, the true strain failure, an indicator of plastic deformation has been reported to be negligible to 373 K (100 °C). The true strain to failure increases to more than 50 pct as the temperature is raised beyond 373 K (100 °C). In addition, it also has been shown by Narita *et al.*[12] that the critical resolved shear stress for the $\{110\}\langle 1\bar{1}0\rangle$ slip decreases from 2 MPa to 0.5 MPa as temperature increases from 77 K to 353 K (–196 °C to

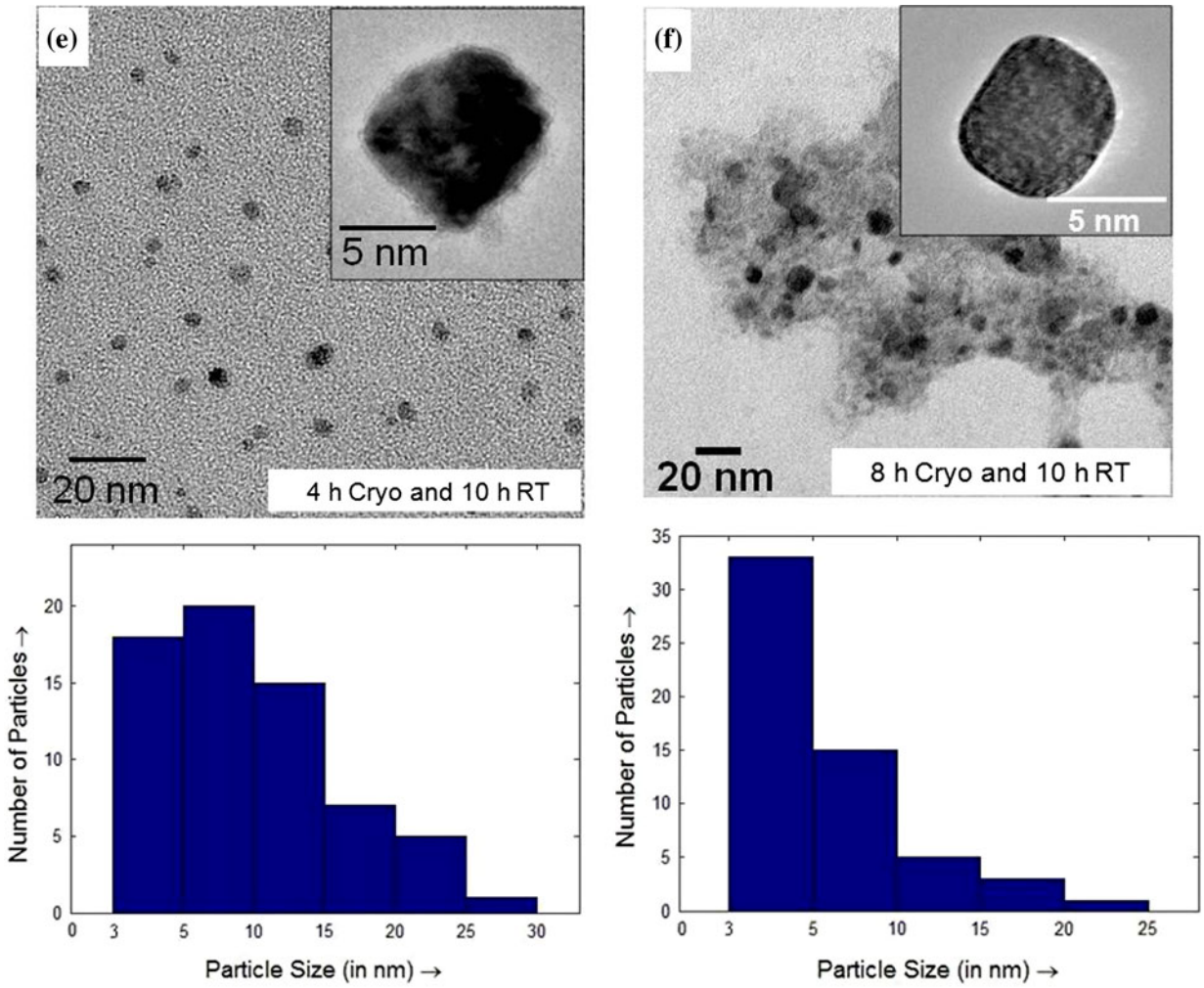

Fig. 4—Continued.

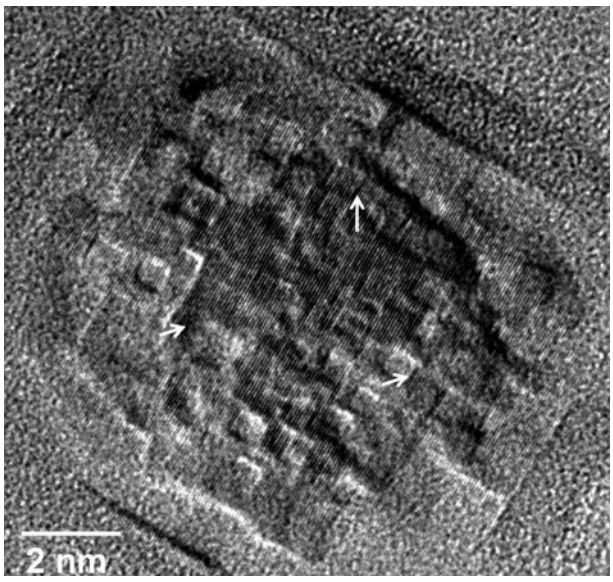

Fig. 5—High-resolution micrograph of a NaCl crystallite prepared by cryomilling for 8 h and subsequently RT milled for 10 h. The presence of defects are marked by arrows.

80 °C). Therefore, it is easier to initiate plastic deformation by ball milling at RT than at cryogenic temperature. These factors clearly suggest that a combined cryo and RT milling will lead to formation of an ultrafine NaCl crystallite. At cryogenic temperatures, little plastic deformation occurs in NaCl crystallites, and failure takes place from defects such as microcracks. Cooling of the powder is the effective means to accelerate this fracturing process. NaCl crystallites (as shown in Figures 2(b) and (c)) reveal little plastic deformation at cryogenic temperature. Figure 6(a) shows high-resolution images obtained from samples cryomilled for 8 hours revealing no visible defect.

During RT milling, NaCl crystallites, it is likely that temperature would increase during a high-energy impact by the balls. Miller *et al.*[15] showed that the local temperature rise for brittle materials such as NaCl could be 673 K to 773 K (400 °C to 500 °C) during continuous milling. It has been suggested by the authors[15] that the observed temperatures are localized in small volumes of the impacted crystals. In the present case, the temperature of the vial has been monitored using a RTD sensor attached to the vial. The peak temperature

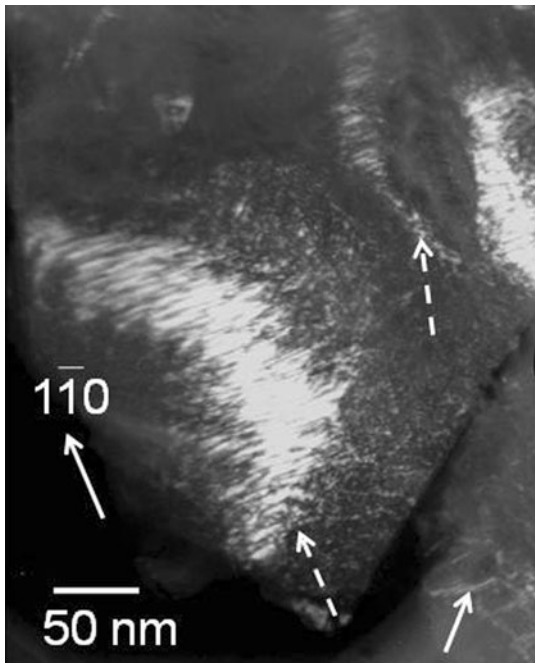

Fig. 6—Dark-field micrograph of a particle obtained with $g = [1\bar{1}0]$ showing the presence of dislocation cells and walls (marked by white arrows). This is obtained from the sample cryo milled for 2 h and subsequently RT milled for 10 h.

recorded is 453 K (180 °C). The milling machine was stopped intermittently to check the vacuum level in the vial. Therefore, the temperature increase in the present case would be much less than that reported by Miller *et al.*[15] It is to be noted that the temperature of the NaCl crystallite under the impact of the ball would be much higher. Schwarz and Koch[16] have analyzed the temperature increase resulting from the localized shear of powder entrapped between the two balls during ball milling and obtained the following equation:

$$\Delta T = \frac{F}{2}\left(\frac{\Delta t}{\pi k \rho C_P}\right)^{1/2} \quad [1]$$

where ΔT = temperature increase, F = dissipated energy flux = $\sigma.V$, where σ = normal stress caused by head-on collision, V = relative velocity of the balls before impact, Δt = stress state lifetime, ρ = powder particle density, k = thermal conductivity of powder, and C_P = heat capacity of powder. We can assume that the normal stress is the maximum compressive stress generated by a head-on collision of two balls of diameter d. Then the normal stress can be calculated using the following equation[17]:

$$\sigma = \sigma_c = 0.616\left\{PE^2\left(\frac{2}{d}\right)^2\right\}^{\frac{1}{3}} \quad [2]$$

where E = elastic modulus of the balls, P = load. Using the values given in Table I and V_r = 20 m/s, the calculated value of ΔT = 728 K = 455 °C. Therefore, it is likely that the temperature of NaCl crystallite during RT ball milling operation would be much higher than brittle-to-ductile transition temperature and thereby would cause plastic deformation. Figure 6 is a dark-field micrograph of a particle prepared by 2 hours of cryomilling followed by 10 hours of RT milling. The presence of dislocation cells are marked by solid white arrows, whereas the low-angle grain boundaries are shown by broken arrows on the figure. The low-angle tilt boundaries are considered to be formed by an array of dislocations. Figure 7(b) (sample cryomilled for 8 hours followed by RT milled for 10 hours) reveals numerous dislocations (marked on the figure). The calculations from various images indicate dislocation density of $1.5 \times 10^{16}/m^2$ in the sample. In addition, the dislocations appear as dipoles as observed in many metals.[10] The dislocation dipoles are dislocation loops with elongation along one direction so that they look like a pair of single dislocations with opposite Burgers vectors. Therefore, the mechanisms responsible for mechanical milling in ductile system now can be applied to RT milling of NaCl powder. RT milling will lead to the localized deformation with shear bands containing a high density of dislocation as evidenced in Figures 6 and 7(b). For continued reduction in crystallite size, an accumulation of dislocation in the microstructure is necessary.[3,4] This accumulation will cause large crystallites to be disintegrated into subgrains separated by low-angle boundaries. The formation of such subgrains requires annihilation and recombination of dislocations leading to decrease in strain. The subgrains are formed by polygonization—low-energy configuration of dislocation of the same sign. Amelinckx and Strumane[18] have studied the kinetics of polygonization in NaCl. These authors have shown that first stage of polygonization (rearrangement of the dislocation in the glide plane) requires the temperature to be at 300 K (27 °C). By studying isothermal growth kinetics of polygonizing domains (being responsible for subgrain formation), these authors have shown that domain growth is slow up to 473 K (200 °C).[18] An appreciable growth of polygonizing domains is observed at a temperature of 673 K (400 °C). Therefore, the temperature-dependent mechanical properties as well as the polygonization kinetics clearly reflect that the preparation of ultrafine nanocrystalline NaCl crystallites requires combined cryo and RT milling.

An important observation of the current study is the bimodal size distribution of NaCl crystallites for samples cryomilled and subsequently RT milled (Figures 2(a) and (b)). It has been observed that the microstructures consist of a few large faceted crystallites with multiple small crystallites. The detailed microstructural observation indicates the formation of numerous

Table I. Some Physical and Mechanical Properties of NaCl

Thermal conductivity of NaCl, k (W/m.K)	4.85[6]
Heat Capacity of NaCl, C_P (J/kg × K)	837.1[6]
Density of NaCl, ρ (Kg/m^3)	2170[19]
Longitudinal wave velocity, V_s (m/s)	3000[20]
Elastic modulus of WC, E (GPa)	704[21]
Density of WC, ρ_{WC}	15.63[22]
WC ball diameter, d (m)	0.015

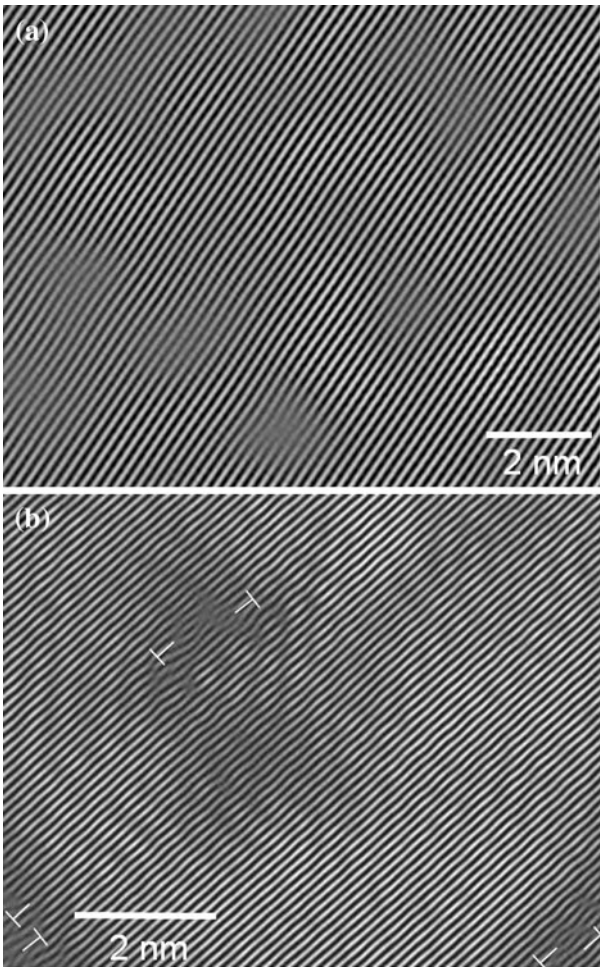

Fig. 7—High-resolution micrograph of a NaCl crystallite prepared (*a*) by cryomilling for 8 h and (*b*) by cryomilling for 8 h and subsequently RT milled for 10 h. The presence of dislocation dipoles are marked on (*b*).

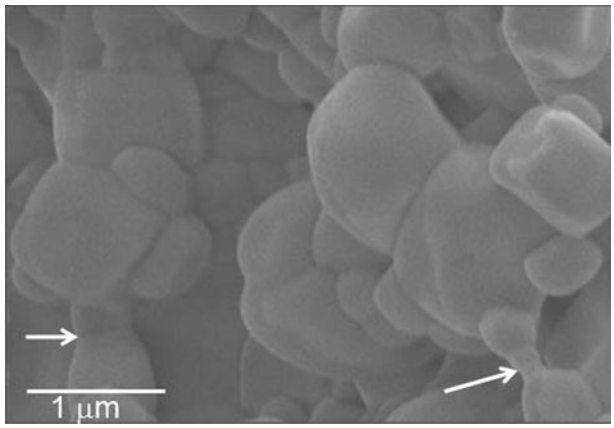

Fig. 8—SEM of NaCl powder cryo milled for 4 h and RT milled for 10 h revealing the formation of neck.

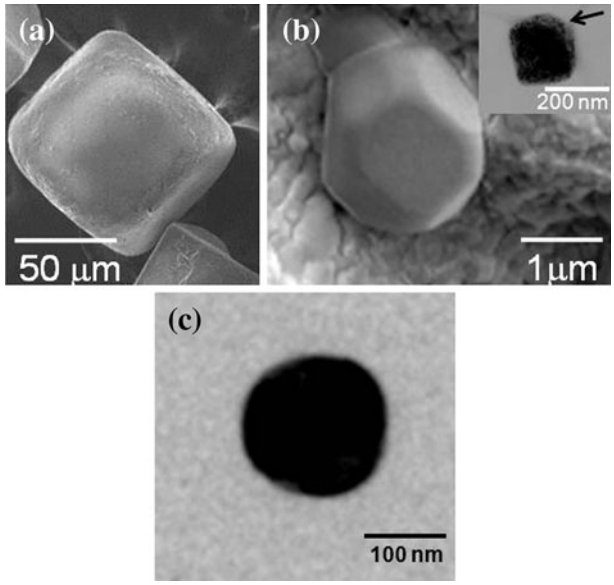

Fig. 9—SEM micrographs of crystallites in (*a*) starting powder; (*b*) cryomilled for 2 h and RT milled for 10 h; (*c*) TEM bright-field micrograph of a crystallite obtained during cryo milling (8 h) and RT milled (10 h). The inset in Fig. 9(b) shows a TEM bright-field micrograph depicting the shape change. The arrow on the figure indicates the roughening of surfaces.

cases of intercrystalline necking. Figure 8 shows a SEM micrograph revealing the formation of few such necks (marked by white arrows). Such observations also have been made by Davis and Koch[20] for brittle couples Si-Ge. This finding can attributed to the sintering of smaller NaCl crystallites to form a larger one. The sintering of NaCl crystallites can occur due to temperature-enhanced plastic deformation as well as microdiffusion during RT mechanical milling. It has been reported in the literature that surface and volume diffusion, plastic deformation and evaporation condensation are three basic mechanisms for the sintering of NaCl crystallites.[6,19,23,24] Morgan *et al.* attributed the densification in the early stage to plastic flow.[23] We already have discussed in the last section that RT milling can lead to a temperature increase of 673 K to 773 K (400 °C to 500 °C). This increase will lead to enhanced plastic deformation as well as diffusion caused by defect generation. After a limited densification caused by plastic yielding, the grain-boundary diffusion has been reported to be the dominant sintering mechanism.[6] The decrease of the crystallite size during mechanical milling leads to a substantial increase in the grain-boundary area, making the grain-boundary diffusion at elevated temperature the dominant sintering mechanism.

Another interesting finding of the present study is the change of the surface morphology of the NaCl crystallites during RT milling. The crystallites in the starting powder have the typical cuboidal morphology (Figure 9(a)) well sharp {100} facets. During RT milling, the shape of the NaCl crystals changes to cuboctahedron (Figure 9(b)) to near spherical (Figure 9(c)). The inset in Figure 9(b) shows a TEM bright-field micrograph of a smaller crystallite depicting the roughening of {100} surfaces. It is well known that at temperatures $T < 923$ K (650 °C), the equilibrium shape of the NaCl crystal is cube with exposed {100}

facets.[25–27] It has been reported that a sharp transition occurs at a temperature $T = 923$ K (650 °C), above which thermal roughening of edges and corners occur. It has been observed[27] that these rounded regions coalesce $T = 993$ K (720 °C) so that no sharp edges between the {100} facets remains. It is to be noted here that thermal roughening in NaCl is exemplified as a class B roughening transition in which the completely faceted shape is stable up to a nonzero temperature ($T = 923$ K [650 °C]).[25] Eventually, as temperature is increased beyond 923 K (650 °C), the facets disappear. In mechanical milling, the temperature of the NaCl crystallite will never reach 923 K (650 °C). There can be two different kinds of temperature effects during mechanical milling.[16,28–32] One is the local temperature pulse, which is caused by ball powder collisions. This kind of temperature pulse has a short duration, approximately the same as that of the collision time between the ball and the powder (10^{-5} seconds).[24] It is difficult to measure this local temperature pulse experimentally. Therefore, it can be estimated theoretically using appropriate models encompassing the extent of plastic deformation the powder particles undergo as well as the extent of heat transfer, which depends on the type of balls and the powder materials. The theoretical calculations (as discussed earlier) indicate that this temperature is approximately 728 K (455 °C). The second kind is the overall temperature increase in the vial, which can be estimated theoretically and measured experimentally. Many experimental measurements have been reported in the literature and the temperature increase has varied between 323 K and 473 K (50 °C and 200 °C).[16] The temperature of the vial has been monitored in the present investigations and the maximum temperature increase recorded is 453 K (180 °C). Therefore, the roughening of NaCl crystallites does not occur due to thermal effects. Rather, this outcome is a clear signature of plastic-deformation-induced surface roughening of NaCl nanocrystals. Plastic deformation has been reported to roughen a free surface by producing among other things, slip bands within the grains along with relative rotation and sliding among grains in case of bulk materials.[33–37] The roughness increases in linear proportion to the magnitude of plastic deformation (strain) and average grain size of the material. Microscopically, the fundamental cause of surface roughening is the dislocation movement. There are reports in the literature on the plastic-deformation-induced surface roughening of KCl during RT plastic deformation.[36] It has been shown that surface roughening starts to occur through a stochastic accumulation of slip events. Figures 5 and 6 reveal the presence of dislocations (marked by white arrows) and surface steps (marked by black arrows on Figure 6) on a nanosized NaCl crystal. It is well known that dislocations generated within the crystals move to the surface to create a surface step. As the amount of deformation increases, accelerated surface roughening takes place by the emergence of persistent wider slip bands. The origin of these slip bands in the mechanical-milled NaCl crystals is under study and will be communicated later.

V. CONCLUSION

In summary, the combined cryo and room-temperature mechanical milling is found to be very effective in the formation of ultrafine NaCl crystallites. This formation has been possible because of a high brittle-to-ductile transition temperature (~540 K [~267 °C]). This can be explained using the temperature-dependent mechanical property of NaCl. The detailed microstructural study using SEM and TEM show several interesting features. The NaCl crystallites undergo plastic-deformation-induced roughening, leading to a change of shape from cuboid to cuboctahedron to nearly spherical. The formation of bigger crystallites can be explained as a result of sintering of smaller NaCl crystallites aided by plastic deformation as well as grain-boundary diffusion.

ACKNOWLEDGMENTS

The authors would like to thank the Department of Science and Technology, India and Nano Science and Technology Initiative (NSTI) for support.

REFERENCES

1. B.S. Murty and S. Ranganathan: *Int. Mater. Rev.*, 1998, vol. 43, pp. 103–41.
2. R.M. Davis, B. McDermott, and C.C. Koch: *Metall. Trans. A*, 1988, vol. 19A, pp. 2867–74.
3. K.H. Chung, J. Lee, R. Rodriguez, and E.J. Lavernia: *Metall. Mater. Trans. A*, 2002, vol. 33A, pp. 125–34.
4. J. Lee, F. Zhou, K.H. Ching, N.J. Kim, and E.J. Lavernia: *Metall. Mater. Trans. A*, 2001, vol. 32A, pp. 3109–15.
5. R.J. Perez, H.G. Jiang, C.P. Dogan, and E.J. Lavernia: *Metall. Mater. Trans. A*, 1998, vol. 29A, pp. 2469–75.
6. L.W. Smiser and T.D. McGee: *J. Amer. Soc.*, 1969, vol. 52 (12), pp. 681–82.
7. R. Goodall, J.F. Despois, and A. Mortensen: *J. Euro. Ceram. Soc.*, 2006, vol. 26, pp. 3487–97.
8. H.J. Fecht: *Nanostruct. Mater.*, 1995, vol. 6, pp. 33–42.
9. F.A. Mohamed: *Acta Mater.*, 2003, vol. 51, pp. 4107–19.
10. E.J. Lavernia, B.Q. Han, and J.M. Schoenung: *Mater. Sci. Eng. A*, 2008, vol. 493, pp. 207–14.
11. B.Q. Han, J. Ye, F. Tang, J. Schoenung, and E.J. Lavernia: *J. Mater. Sci*, 2007, vol. 42, pp. 1660–72.
12. N. Narita, Y. Takahara, and K. Higashida: *Phil. Mag. A*, 2002, vol. 82 (17–18), pp. 3229–39.
13. S.A. Long and T.D. Mcgee: *J. Am. Ceram. Soc.*, 1963, vol. 46 (12), pp. 583–87.
14. S.M. Wiederhorn, R.L. Moses, and B.L. Bean: *J. Am. Ceram. Soc.*, 2006, vol. 53, pp. 18–23.
15. P.J. Miller, C.S. Coffey, and V.F. DeVast: *J. Appl. Phys.*, 1986, vol. 59, pp. 913–16.
16. R.B. Schwarz and C.C. Koch: *Appl. Phys. Lett.*, 1986, vol. 49, pp. 146–48.
17. R.J. Roark: *Formulas for Stress and Strain*, McGraw-Hill, New York, NY, 1954, p. 275.
18. S. Amelinckx and R. Strumane: *Acta Metall.*, 1960, vol. 8, pp. 312–20.
19. W.D. Kingery and M. Berg: *J. Appl. Phys.*, 1988, vol. 26 (10), pp. 1205–12.
20. R.M. Davis and C.C. Koch: *Scripta Mater.*, 1987, vol. 21, pp. 305–10.
21. H. Doi, Y. Fuhiwara, K. Miyake, and M. Oosawa: *Metall. Trans.*, 1970, vol. 1, pp. 1417–25.
22. P.K. Deshpande, J.H. Li, and R.Y. Lin: *Mater. Sci. Eng. A*, 2006, vol. 429, pp. 58–65.

23. C.S. Morgan, L.L. Hall, and C.S. Yust: *J. Amer. Soc.*, 1963, vol. 46 (11), pp. 559–60.
24. J.B. Moser and D.H. Whitmore: *J. Appl. Phy.*, 1960, vol. 31 (3), pp. 488–93.
25. A-C. Shi and M. Wortis: *Phys. Rev. B*, 1988, vol. 37 (13), pp. 7793–7805.
26. J.C. Heyraud and J.J. Metois: *J. Cryst. Growth*, 1987, vol. 84, pp. 503–08.
27. P.A. Mulheran: *Model Simul. Mater. Sci. Eng.*, 1994, vol. 2, pp. 1123–29.
28. A.K. Bhattacharya and E. Arzt: *Scripta Metall.*, 1992, vol. 27, pp. 749–54.
29. R.M. Davis and C.C. Koch: *Scripta Metall.*, 1987, vol. 21, pp. 305–10.
30. T.H. Courtney: *Mater. Trans. JIM*, 1995, vol. 36, pp. 110–22.
31. R.M. Davis, B. Mcdermott, and C.C. Koch: *Metall. Trans.*, 1988, vol. 19A, pp. 2867–74.
32. T.H. Courtney: *Rev. Part. Mater.*, 1994, vol. 2, pp. 63–116.
33. J. Villain, D.R. Grempel, and J. Lapujoulade: *J. Phys. F: Met. Phys.*, 1985, vol. 15, pp. 809–34.
34. E.H. Conrad and T. Engel: *Surf. Sci.*, 1994, vol. 299 (300), pp. 391–404.
35. Y.Z. Dai and F.P. Chiang: *Trans. ASME*, 1992, vol. 114, pp. 432–38.
36. E.M. Nadgorny, J. Schwerdtfeger, F. Madani-Grasset, V. Kontsos, E.C. Aifantis, and M. Zaiser; *Proc. Int. Conf. on Statistical Mech. of Plasticity and Related Instabilities, Proc. of Sci.*, 2005, pp. 1–11.
37. M. Zaiser, F. Madani-Grasset, V. Koutsos, and E.C. Aifantis: *Phy. Rev. Lett.*, 2004, vol. 93, pp. 195507-1–195507-4.